

Comprehensive optical study of CdS and Fe/CdS nanoparticles synthesized by laser ablation

Angham Shihab Ahmed* , Ahmed Baqer Sharba ,
Qussay Mohammed Salman 

University of Babylon, College of Science for Women, Department of Laser Physics, Babylon, Iraq.

*Corresponding author: angham.harbi.gsci168@student.uobabylon.edu.iq

Original Research

Abstract:

Received:
4 November 2024
Revised:
13 November 2024
Accepted:
17 November 2024
Published online:
30 December 2024

This work presents a detailed study of the characteristics of CdS and Fe/CdS nanoparticles synthesized by pulsed laser ablation in liquid at different conditions (environment, fluence, concentration). The study shows and discusses the crucial conditions and parameters that influence the production of the CdS and Fe/CdS nanoparticles. The results showed that the size and size distribution of CdS nanoparticles in methanol depends significantly on the particle concentration, laser fluence, and the liquid type. In addition, the presence of Fe nanoparticles in methanol limits the production of CdS to ultra-small particles even at high concentrations without affecting the structure of the energy states of the CdS nanoparticles. CdS nanoparticles generated in water suffer from the effects of water molecules, especially at low concentrations. This effect does not involve a permanent change in the composition of the particles. Adding surfactants to water reduces or eliminates these effects and significantly increases the ablation efficiency. The presence of CdS, Fe, and Fe/CdS in methanol does not noticeably affect the refractive index, chromatic dispersion, and thermal properties of the liquid. The results of this study can guide the process of controlling the properties of pure and hybrid CdS nanoparticles for optoelectronic and photonic applications.

© The Author(s) 2024

Keywords: CdS nanoparticles; Fe/CdS nanoparticles; Pulse laser ablation; Optical properties

1. Introduction

A large number of studies have been devoted to find new materials with superior performance in optoelectronics and optical applications [1–5]. Although many proposed materials are available, the challenges associated with their production, high cost, toxicity, and difficulty of use in systems constitute major obstacles to the progress of optoelectronics. Semiconductors are among the most promising materials in this field, as semiconductors have a crucial role in developing modern optoelectronic devices and various optical applications [1, 6, 7]. II-VI semiconductors in various nano-scale structures have multiple scientific and technological applications. Among these materials, cadmium sulfide (CdS) is a promising binary semiconductor, used in a variety of optical and electronic applications [8]. It has a wide energy band gap and very low solubility in water, unlike its rapid solubility in acids [9]. The activity of nanomaterial in different applications, e.g.

photocatalytic, depends on the phase structure and exposed sides of the crystal. In addition, different shapes of nanomaterial affect the material properties due to the different surface-to-volume ratios [10, 11]. Therefore, providing different crystalline forms and different nanostructures can provide different activities for different applications. Furthermore, hybridization of materials is one of the most important ways to obtain materials with new and improved properties. Many studies have proven that very significant improvements can be achieved by hybridizing materials of different characteristics [1–5, 12, 13]. Among these studies, a large number of studies dealt with the hybridization of CdS with iron or one of its oxides, for example [1, 4, 5, 14–18]. This type of hybridization can add magnetic control to nanoparticles in addition to improving the optical and electronic properties of the nanoparticles. Most studies on the phase transformation of CdS crystals are limited to preparation under strict conditions such as

high pressure or high temperatures [10]. In addition, most of the previous studies that adopted the manufacture of pure CdS particles or hybridized with other materials relied on chemical methods [1, 2, 4, 5, 8, 14–17, 19]. In addition, other studies relied on pulsed laser ablation technology to prepare pure CdS nanoparticles and hybridize them with other materials [18, 20–25]. Pulsed laser ablation (PLA) is a very important technique in producing nanomaterial free of impurities with controllable properties [18] and high stability in environmentally friendly conditions. In addition, the laser ablation technique is available for a very wide range of materials, including semiconductors [20, 26].

The technique of analyzing the optical properties of materials upon their interaction with electromagnetic radiation provides highly valuable information about the physical and chemical properties of the material. These optical properties include absorption, emission, reflection, refraction, diffraction, and scattering. For semiconductors, the optical properties are related to the characteristics of the energy bands and the atomic structure of the substance [27]. Studies of the optical absorption edges of semiconductors provide important information about the states near the valence band and conduction band, in addition to the forbidden energy band gap. This information is essential for determining the performance of semiconductors in different applications [4, 9, 17].

In this work, we presented a detailed optical study on pure CdS and Fe/CdS nanoparticles synthesized using the PLA technique in liquid with different preparation conditions. The study included a detailed investigation into the properties of the nanoparticles generated in methanol and water in terms of size, energy gap, aggregation rate, and interaction with liquid molecules. In addition, the effects of laser parameters, particle concentration, and the presence of iron nanoparticles on the characteristics of the CdS nanoparticles were studied. The study presents the main parameters that influence the properties of CdS and Fe/CdS particles and discuss the physical and chemical origin of these parameters. Furthermore, this work shows the advantages of PLA and the properties of hybridization that cannot be achieved by chemical route. Moreover, we presented the effects of the generated particles on the linear refraction and the thermal and dispersion properties of the liquid.

2. Experimental part

At the beginning 20 mm diameter discs of CdS and Fe were fabricated by mechanically pressing CdS and Fe micro-scale powders, respectively, by using a homemade (30 MPa) hydraulic pressing device. The samples of Fe, CdS, and Fe/CdS were prepared at different concentrations in water and methanol by using pulsed laser ablation with an Nd:YAG laser at a wavelength of 1064 nm, a pulse duration of 4.5 nsec, a repetition rate of 4 Hz, and different energy densities ($1.4 - 13.3 \text{ J/cm}^2$). In all the preparation processes, the samples were immersed in 10 mL of liquid, where the surface of the targets was at 6 mm below the liquid surface. The fluence of the laser beam on the surface of the target was ($1.4 - 13.3 \text{ J/cm}^2$). The pulse energy was measured by a Gentec-EO joule meter.

To prepare the Fe/CdS sample, Fe particles were first prepared by firing the iron target in water or methanol with laser pulses. After that, the iron target was removed and replaced with the CdS target, and the laser ablation process was repeated. After completing the preparation process, an external magnetic field was used to separate the generated particles. Using this method, all the CdS particles that are not connected with iron particles were eliminated. To prepare the CdS/Fe sample, the same method above was used, but the CdS particles were first prepared in the liquid. CdS nanoparticles were also synthesized in water with different concentrations of Cetyltrimethylammonium bromide (CTAB) and different concentrations of polyvinyl alcohol separately. The prepared CdS samples were 8 samples in methanol, 8 samples in pure water, 3 samples in water with CTAB, and 3 samples in water with PVA. In addition, 3 samples of Fe/CdS were prepared in methanol and 3 samples in water. Two addition samples of CdS/Fe were synthesized in methanol.

The processes of determine the exact concentration of the nanoparticles prepared by PLA are not direct jobs and do not usually have the reliable accuracy. Instead, in this work we depended on the number of the laser pulses used and the absorbance intensity for indicating the relative concentrations of the samples. This method is fairly enough, since we are interested in showing the effects of changing some preparation conditions relative to the effects of other preparation conditions.

Absorption spectra were measured over the range of 190–900 nm using a CECIL CE7200 UV/VIS spectrophotometer. To measure the linear refractive index, the experimental setup described in reference [6] was used. The refractive index and its thermal coefficient were measured at three wavelengths (405, 532, and 632.8 nm). The refractive index of the samples was measured with an accuracy of 3.5×10^{-5} .

3. Results and discussion

3.1 Laser ablation in methanol

Figure 1 presents images of samples of Fe, CdS, Fe/CdS, and Fe/CdS before eliminating the CdS particles that are

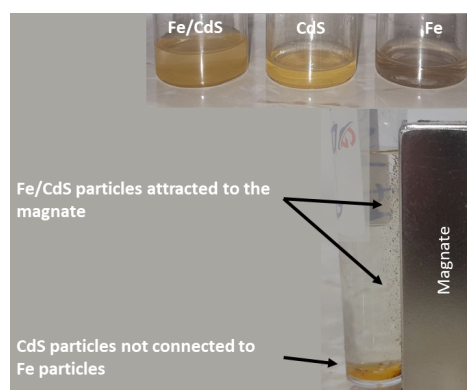


Figure 1. Images of samples of Fe, CdS, Fe/CdS, and as prepared Fe/CdS sample before eliminating the CdS particles that are not connected to Fe.

not connected to the Fe particles. The figure shows how the Fe/CdS particles are attracted to the external magnet. Figure 2 presents some SEM images of the samples of the study. These images are examples showing the size scale of the produced nanoparticles. The statistics of the SEM images showed that the Fe and CdS particles are spherical

or semispherical particles with size ranging between 5 – 50 nm. At the stage of SEM sample preparation, the CdS nanoparticles prepared in methanol form large scale random aggregates. However, CdS prepared in water structured in large scale cubes at the stage of particles creation. Fe nanoparticles prepared in water and methanol are normally

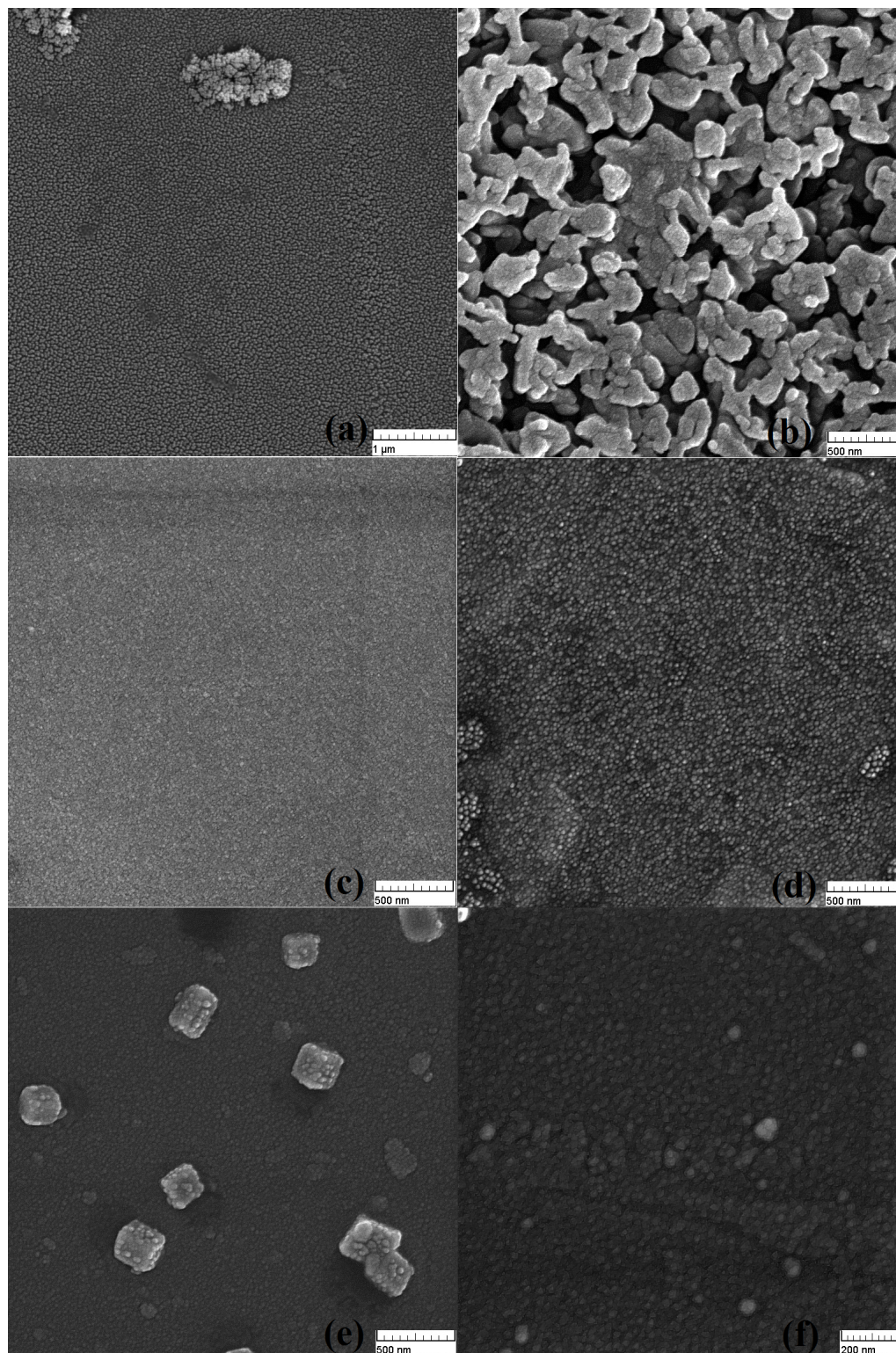


Figure 2. (a-c) SEM images of Fe, CdS, Fe/CdS samples prepared in methanol, respectively, and (d-f) of Fe, CdS, Fe/CdS samples prepared in water.

covered with a layer of Iron oxide.

Studying the optical characteristics of nanoparticles can clarify most of the physical and chemical properties of the particles and their interactions with the environment. Figure 3 (a) shows the absorption spectra of CdS nanoparticles prepared in methanol by laser ablation at different pulse numbers with (1.4 J/cm^2) energy density on the target surface.

As can be seen from Figure 3 (a), the absorption spectra of the samples prepared with number of pulses (30 and 60 pulses) consist of a sharp band with a peak at 250 nm and a broad absorption band peaked at 300 nm and extending to most of the visible region. This indicates the formation of nanoparticles with different size distributions. The sharp peak in the ultraviolet region indicates the formation of CdS nanoparticles with sizes less than 2 nm (according to an effective mass approximation based relation [28]) with a very narrow size distribution. The appearance of this sharp peak indicates the formation of particles with a certain preferential or “magical” agglomeration number [29]. Depending on the absorbance value, it becomes clear that, the percentage of particles formed with the preferential aggregation number is higher than the other sizes formed in the sample. When the number of laser pulses increases to 300 pulses, that is, the concentration of the formed particles increases, the two absorption regions merge together, with the peak at 250 nm remains the highest in the absorption spectrum. This reveals an increase in the width of the size distribution of the particles due to an increase in the aggregation or the agglomeration rate of particles in the liquid when their concentration increases. The aggregation of CdS particles indicates that the surfaces of these particles are free of

surface charge. However, by preparing samples of CdS particles at very high concentrations, it was found that the size of the final particles remains within the range of nanoparticles (10 – 40 nm).

The fluence of the laser used has a direct effect on the properties and quantity of nanomaterial produced in the liquid. Figure 3 (b) shows the absorption spectra of two samples prepared at different energy densities. The energy density was calculated on the surface of the target. From the figure, it can be seen that, as the fluence increases, the sharp peak region is shifted towards longer wavelengths (from 250 nm to 280 nm). This indicates that the average size of the particles increases with the increase in laser fluence. This increase in size happens at the stage of particle creation and not at the post-synthesis stages, as will be explained below. Figure 3 (b) also shows that the efficiency of laser ablation decreases considerably as the laser fluence increases. Particle size and size distribution increasing with the increasing of laser fluence have also been observed in some previous works, e.g. [30, 31].

Determining the mechanisms of laser fluence effect on the properties of nanomaterial and specifying the contribution of each mechanism is a very complicated task. That is, in the laser ablation process, the properties of nanomaterial depend on the set of interactions that occur from the moment the laser pulse falls on the surface of the target until the end of the nanoparticle formation process. These processes include surface absorption of photons, formation of plasma on the surface, expansion of the formed plasma, formation of cavitation bubbles, formation of shock waves, interaction of the formed plasma with the rest of the laser pulse, particle nucleation, and cooling of the plasma. All these

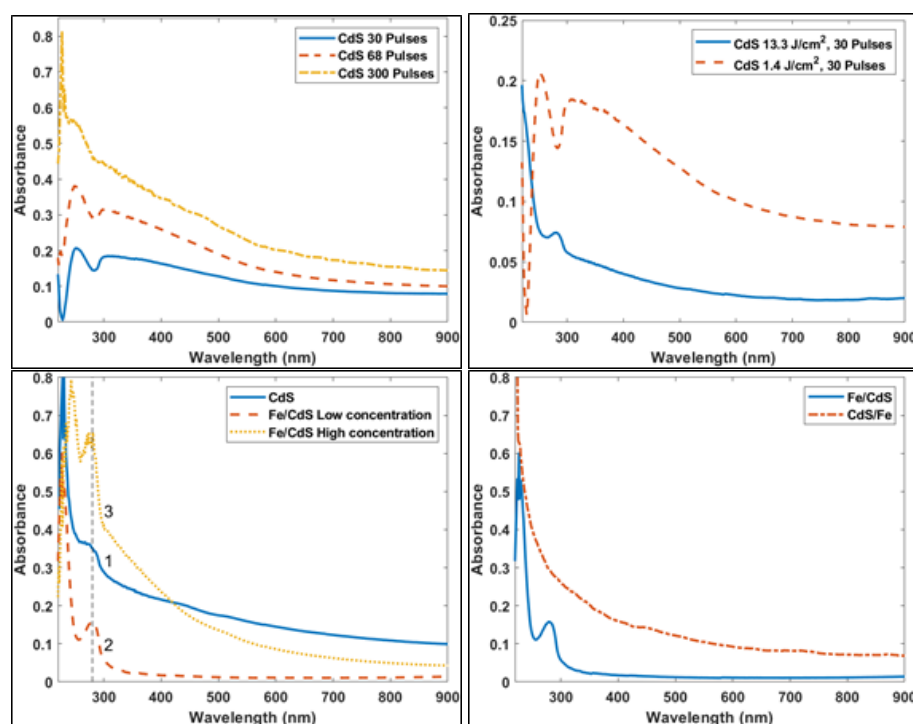


Figure 3. Linear absorption spectra of nanoparticles prepared in methanol (a) CdS prepared at the same laser energy (b) CdS prepared at different laser energy values, (c) CdS and Fe/CdS, and (d) Fe/CdS and CdS/Fe.

processes depend on the laser parameters and the physical and chemical properties of the liquid and the target material [32–34]. One of the most important processes that cause the average size of nanoparticles to increase with the increase in laser intensity used is the direct effect of laser intensity on the thermodynamics of the formed plasma and cavitation bubbles. Higher laser fluence leads to raising the temperature and pressure of the formed plasma, which means a longer lifetime for the cavitation bubbles. This leads to the formation of larger nanoparticles [32, 35]. In addition, the formation of plasma at higher fluence leads to an increase in the effect of the plasma shield formed on the surface of the target. This results in a decrease in the amount of light energy reaching the surface of the target [36], which directly affects the size of the particles formed and the efficiency of the ablation process [37, 38]. Moreover, increasing the laser fluence can cause optical collapse of the laser beam in the focal area, which causes a significant decrease in the energy reaching the surface of the sample, hence, affecting the size and quantity of nanomaterial created in the liquid [33]. However, the dependence of the size of the particles on the laser fluence enables a very simple and effective tool to produce nanoparticles with controllable size.

Bulk CdS material has an energy gap of about 2.42 eV [4]. In the nano-scale, the energy gap increases as the particle size decreases due to quantum confinement effects [39]. CdS nanoparticles synthesized in methanol have an energy gap much larger than the energy gap of the bulk material. This denotes the formation of particles with radii close to or less than the Exciton Bohr radius. Table 1 contains examples of the energy gap value for samples prepared with different pulse numbers. The energy gap was calculated from the absorption spectrum using Tauc's formula [17] for direct allowed transitions.

The values of the energy gap shown in the table are not always constant for the samples prepared with the same number of pulses but rather depend on the energy density of the laser and the type of liquid. However, the energy gap was calculated here to show that its value decreases with the increase in the number of laser pulses, which indicates an increase in the size of the CdS particles.

Laser ablation of CdS in methanol containing iron nanoparticles reveals other important properties of this compound. The absorption spectra in Figure 3 (c), curves 1, 2, and 3, are for CdS particles prepared in pure methanol, CdS particles prepared in methanol containing iron nanoparticles, and CdS particles prepared at a high concentration in methanol containing a high concentration of iron nanoparticles, respectively. Comparing curve 1 with curve 2 shows a very important result. Curve 1 contains a shoulder in the ultraviolet region indicating the formation of CdS particles of very small sizes (smaller than 2 nm) and a wide absorption band covering the visible and near-infrared region representing the absorption of a wide size distribution. However, curve 2 contains a very sharp band with a peak at 280 nm with near zero absorbance in the visible and near infrared region. This result reveals that the CdS particles formed on the iron particles are of very small sizes and with a very narrow size distribution. In other words, the presence of iron particles

Table 1. The optical energy gap of CdS nanoparticles prepared in methanol by pulsed laser ablation method with different number of pulses.

Material	No. of Pulses	Eg (eV)
CdS	775	3.95
CdS	1700	3.85
CdS	2700	2.7

prevents the aggregation of CdS particles. This case remains valid even at high concentrations of the CdS nanoparticles, as can be observed from curve 3, which contains a sharp peak at 280 nm representing the generation of CdS particles of the same size as those generated at low concentrations. The absorbance at the beginning of the visible region in this curve is due to the iron particles, as it exactly matches the absorption spectrum of pure iron nanoparticles (not drawn). The role of the iron nanoparticles in preventing the CdS aggregation was also confirmed by SEM examination, as shown in Figure 2 (c).

In addition, the appearance of the absorption peak at 280 nm, curves 1 and 2, suggests that the clustering of CdS nanoparticles on the iron nanoparticles does not change the energy gap value of CdS. It also does not change the preferential agglomeration number of these particles. This means that the structure of the energy levels and charge distribution of the CdS particles is not affected upon bonding to the iron nanoparticles. This is different from the case of Fe-doped CdS nanoparticles prepared by chemical methods [1, 17], where the energy states of the Fe ion interfere with those of CdS. This fact, along with the generation of a narrow distribution of CdS nanoparticles without any capping agent, can be considered an important advantage of generating Fe/CdS nanoparticles by laser ablation method in methanol.

Figure 3 (d) shows another mechanism of the assembly of iron and CdS particles. For this sample, the CdS nanoparticles were first prepared in methanol, after that, the iron nanoparticles were ablated in the sample. As can be seen from Figure 3 (d), the absence of the sharp peak in the ultraviolet region declares the formation of relatively large size CdS nanoparticles. However, this did not prevent the adhesion of iron particles on these CdS nanoparticles. This result indicates that the improvement of aggregation properties of CdS gained by the presence of iron particles occurs in the initial stages of the formation of the CdS particles and not in the post-formation stages. It also confirms the possibility of adding the magnetic control property to CdS nanoparticles of any size.

3.2 Laser ablation in water

CdS particles generated in water exhibit special characteristics that are completely different from those generated in methanol. Figure 4 (a) shows the absorption spectra of samples of CdS particles prepared in water using different numbers of pulses.

For samples of low concentrations, i.e. prepared with

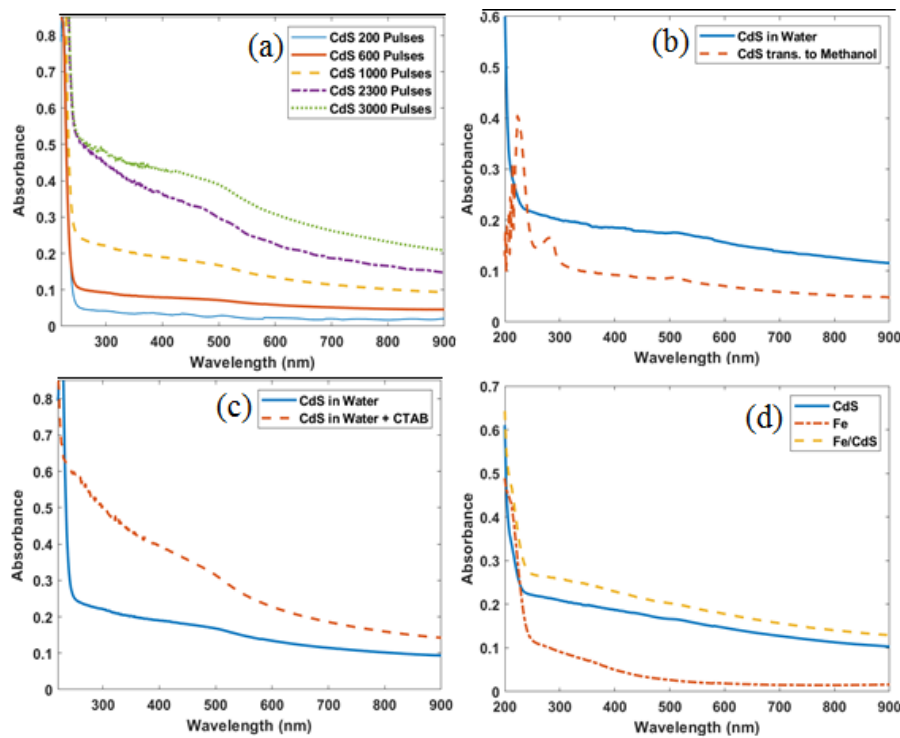


Figure 4. Linear absorption spectra of (a) CdS prepared with different laser pulses number in water (b) CdS prepared in water and transferred to methanol (c) CdS prepared in different liquids (d) CdS, Fe, and Fe/CdS prepared in water.

200 – 1000 pulses, the absorption spectrum shows a very sharp edge in the ultraviolet region without any distinctive feature or absorption peak in the other spectral regions. When the concentration increases to relatively high values, the characteristic absorption edge of CdS appears in the visible region. The appearance of the absorption with these characteristics can be due to several reasons that are not easy to distinguish. First, at low concentrations (200 – 1000 pulses), the sharp absorption edge can suggest the formation of very small nanoparticles. When the concentration increases, the aggregation of CdS particles leads to the production of relatively large particles, leading to a red shift of the absorption edge. The formation of relatively large aggregates of CdS in the form of cubic crystals was confirmed by SEM examination shown in Figure 2 (e).

Second, shining laser pulses into water to generate CdS particles can be accompanied by the generation of OH radicals. These radicals attack the CdS particles, leading to the generation of a compound that is unable to absorb for a period that depends on the concentration and size of the particles. Also, the attack of these radicals leads to a reduction in the concentration of CdS particles. After that, S^- radicals are generated, which are responsible for absorption in the visible region upon charge transfer to an unoccupied state in the nanoparticle [29, 40]. This means that, at low concentrations, the attack of OH and the low concentration of S^- may lead to very weak absorbance in the visible region. Increasing the concentration of the particles and increasing their size lead to an increase in the concentration of the S^- radical and an increase in the number of unoccupied states in the particles. This leads to raise the spectral activity and consequently the appearance of the absorption

edge in the visible region.

Third, for nano-scale particles, 40% of the atoms and the molecules are on the surface of the particle [41]. This means that they are in direct contact with the highly polar water molecules which can easily accumulate around the particles and may form hydrogen bonds. This can alter the charge distribution on the surface of the small nanoparticles, which can consequently lead to a change in the transition probability and/or the production of electron-hole pairs. This effect depends on the size of the particles since the ratio of surface area to volume and the surface charge distribution are size-dependent. This can explain the significant changes in the absorption properties of the CdS nanoparticles suspended in water depending on their sizes.

To clarify the effect of water molecules on the optical properties of CdS particles, a sample of CdS nanoparticles prepared in water was completely dried and transferred to methanol. The particles were redistributed in methanol using a 200 W sonication device. The absorption spectra of these particles in water and methanol are shown in Figure 4 (b). The difference in the absorbance values in the visible and near-infrared region of the two spectra is caused by the decrease in particle concentration due to drying and transporting processes. We note from the figure that the absorption spectrum of CdS particles in water contains only a sharp edge in the ultraviolet region. However, the absorption spectrum of the same particles in methanol shows a sharp absorption band peaked at 280 nm, which represents the formation of the preferential aggregation number for the CdS particles. This result reveals the strong effect of the polar water molecules on the spectral properties of the CdS nanoparticles. In addition, this result proves that water

molecules do not induce a permanent effect that leads to a change in the composition of the CdS particles but rather a temporary effect caused by the presence of polar water molecules around the nanoparticle.

To further clarify the effect of water molecules, we synthesized CdS nanoparticles in water containing 15.6 mM of CTAB. Figure 4 (c) shows the absorption spectra of two samples of CdS nanoparticles prepared in distilled water and water containing CTAB by using 1000 laser pulses for each. Comparing the two spectra shows that the absorption in the visible region of the sample containing CTAB is much higher than that of the sample prepared without CTAB. This result may be either because CTAB coats the CdS particles, isolating them from the influence of water molecules, which leads to an increase in the optical activity of the particles, or because the presence of CTAB enhances the efficiency of laser ablation, which leads to a higher concentration of the particles. What is worth mentioning is that increasing the concentration of CTAB does not lead to noticeable changes in the properties of the generated CdS nanoparticles.

In addition, CdS nanoparticles were also generated in water containing PVA polymer at a concentration of (0.8 mM). Adding PVA polymer to the preparation liquid leads to almost the same results as those with the CTAB but to a lesser extent. Moreover, the absorption spectra of CdS nanoparticles prepared in water containing PVA by using 265 pulses (not shown) contain a sharp peak at 280 nm, which indicates the preferential aggregation number of these particles.

Figure 4 (d) shows the absorption spectra of Fe and CdS nanoparticles generated in pure water and CdS nanoparticles generated in water containing Fe nanoparticles. What can be observed from the figure is that the presence of iron nanoparticles did not lead to noticeable changes in the absorption spectrum other than adding the absorbance of iron nanoparticles to the total absorbance of the sample. That is, the presence of iron particles did not change the aggregation properties of the CdS nanoparticles nor prevent the effect of water molecules on them. A similar result was obtained in [42].

3.3 Linear refractive index measurements

One of the most important parameters that must be determined when using optical materials in the field of photonics is the index of refraction and its dependence on temperature

and wavelength. To study these parameters, the refractive index of pure methanol, Fe, CdS, and Fe/CdS nanoparticles in methanol was measured with an accuracy of 3.5×10^{-5} by using the experimental setup described in [6]. Figure 5 (a) shows the change in refractive index of these samples with wavelength.

As shown in Figure 5 (a), the presence of Fe, CdS, and Fe/CdS nanoparticles in methanol does not impose any noticeable change in the refractive index of the liquid or the chromatic dispersion $dn/d\lambda$. It can also be noticed that this fact is true in the regions of weak and high absorption of the sample. This means that the presence of these nanoparticles and the charge distribution on their surfaces do not affect the polarization properties of the liquid. In other words, the presence of these nanoparticles in methanol does not change its level of response to the electric field component of the incident light. This result was proven for samples with optical transmittance of about 30%, i.e. containing nanoparticles at high concentrations. This declares that all applications that can employ these nanoparticles do not face the problem of changing the refractive index or the problem of chromatic dispersion differences. This advantage is very important, especially for complex optical systems that sometimes require adding additional components to the system. In addition, it can be observed that the hybridization of CdS nanoparticles with Fe nanoparticles did not affect the refractive properties of the sample. This feature demonstrates that the presence of the Fe nanoparticles, which enables the magnetic control feature of the CdS nanoparticles and improves their aggregation properties, does not impose any significant effect on the refractive properties of the sample.

Figure 5 (b) shows the rate of change of refractive index with temperature (dn/dT) for Fe, CdS, and Fe/CdS nanoparticles at different wavelengths. We notice from the figure that there is a very slight change in the dn/dT rate for methanol in the presence of these nanoparticles. The most obvious change in the value of this parameter occurs at the end of the visible region, the region of weak absorption of the samples. This result reveals the slight effect of the presence of these nanoparticles on the thermal properties of the liquid. The largest change in the value of dn/dT is for the Fe/CdS sample. This could be due to the small size and narrow size distribution of these particles, as indicated in Figure 2 (c and f) and Figure 3 (c and d). For the same value of linear

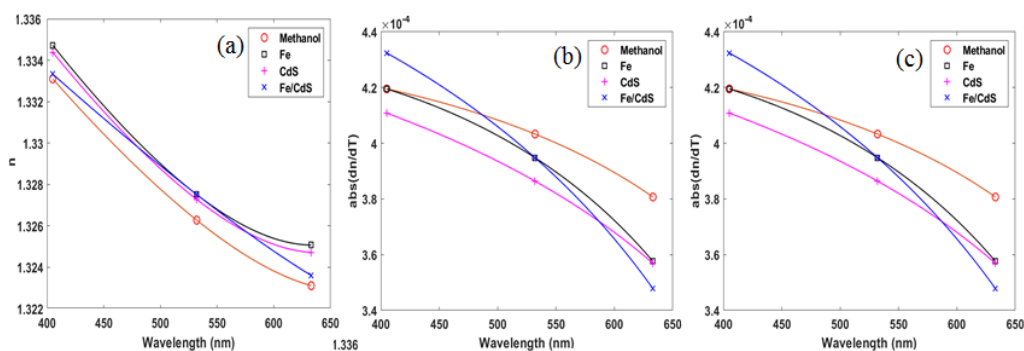


Figure 5. (a) linear refractive index and (b) dn/dT at different wavelengths of pure methanol, Fe, CdS, and Fe/CdS nanoparticles suspended in methanol.

absorbance, the smaller the size of the nanoparticles and the narrower their distribution, the larger their number is. The larger distribution in the liquid and the larger surface area-to-volume ratio mean a larger interface area between the particles and the liquid molecules, which can lead to greater interaction and greater effect.

In general, changing the value of dn/dT has a direct effect on the thermal nonlinear refraction properties of materials [43, 44]. This means that, at the same linear absorbance, the samples under study have the same value of the thermal nonlinear refractive index. Furthermore, the results indicate that the advantage of adding iron to CdS particles does not include significant changes in the thermo-optical properties of the sample. In addition, it can be seen from Figure 5 (b), that the rate of change of dn/dT with wavelength ($dn^2/d\lambda dT$) is the same for all samples. This states that the chromatic properties of the medium are weakly affected by the presence of these nanoparticles.

4. Conclusion

This work presents a detailed optical study on CdS and Fe/CdS nanoparticles both synthesized using laser ablation technique. The study shows the wide divergence of the properties of these particles depending on the preparation conditions. CdS nanoparticles prepared in methanol with low laser fluence have ultra-small size (less than 2 nm) with a very narrow size distribution. The size and the size distribution increase noticeably by increasing the number of laser pulses and by increasing the laser fluence. Increasing the laser fluence also leads to a significant decrease in the ablation efficiency. If Fe nanoparticles are initially present in methanol, CdS nanoparticles can be formed with the preferential aggregation number even at high concentrations without affecting their physical and optical properties. The properties of water molecules and the OH radicals severely affect the size and optical properties of CdS particles generated in water. This effect does not impose permanent structural changes and depends on the concentration of the nanoparticles. It stays the same when Fe particles are present but can be eliminated or reduced by adding a type of surfactant material. In addition, the presence of CdS and Fe/CdS nanoparticles in methanol does not lead to significant changes in the value of the linear refractive index, the chromatic dispersion, and the thermal properties of the liquid.

Authors contributions

Angham Shihab Ahmed: investigation, methodology development, writing the manuscript draft, data analysis and interpretation. Ahmed Baqer Sharba: investigation, reviewing the draft, data validation and verification, and data analysis. Qussay Mohammed Salman: verification, reviewing final manuscript and data analysis, editing, and overall coherence.

Availability of data and materials

The data that support the findings of this study

are available from the corresponding author upon reasonable request.

Conflict of interests

The author declare that they have no known competing financial interests or personal relationships that could have appeared to influence the work reported in this paper.

Open access

This article is licensed under a Creative Commons Attribution 4.0 International License, which permits use, sharing, adaptation, distribution and reproduction in any medium or format, as long as you give appropriate credit to the original author(s) and the source, provide a link to the Creative Commons license, and indicate if changes were made. The images or other third party material in this article are included in the article's Creative Commons license, unless indicated otherwise in a credit line to the material. If material is not included in the article's Creative Commons license and your intended use is not permitted by statutory regulation or exceeds the permitted use, you will need to obtain permission directly from the OICC Press publisher. To view a copy of this license, visit <https://creativecommons.org/licenses/by/4.0>.

References

- [1] M. Junaid, M. Imran, M. Ikram, M. Naz, M. Aqeel, H. Afzal, H. Majeed, and S. Ali. "The study of Fe-doped CdS nanoparticle-assisted photocatalytic degradation of organic dye in wastewater.". *Applied Nanoscience*, **9**:1593–1602, 2019. DOI: <https://doi.org/10.1007/s13204-018-0933-3>.
- [2] C. Tingting, H. Gao, G. Liu, Z. Pu, S. Wang, Z. Yi, X. Wu, and H. Yang. "Preparation of core-shell heterojunction photocatalysts by coating CdS nanoparticles onto Bi₄Ti₃O₁₂ hierarchical microspheres and their photocatalytic removal of organic pollutants and Cr (VI) ions. ". *Colloids and Surfaces A: Physicochemical and Engineering Aspects*, **633**:127918, 2022. DOI: <https://doi.org/10.1016/j.colsurfa.2021.127918>.
- [3] F. Jamal and. A Rafique, S. Moeen, J. Haider, W. Nagan, A. Haider, M. Imran, G. Nazir, M. Alhasan, M. Ikram, Q. Khan, G. Ali, M. Khan, W. Ahmad, and M. Maqbool. "Review of metal sulfide nanostructures and their applications. ". *ACS Applied Nano Materials*, **6**:7077–7106, 2023. DOI: <https://doi.org/10.1021/acsanm.3c00417>.
- [4] A. M. Mansour, R. S. Ibrahim, and A. Azab. "Structure, morphology, optical and magnetic studies of Fe₃O₄-doped CdS nanocomposite. ". *Journal of Materials Science: Materials in Electronics*, **33**:10251–10258, 2022. DOI: <https://doi.org/10.1007/s10854-022-08013-2>.

- [5] A. Rafiq, M. Imran, M. Aqeel, M. Naz, M. Ikram, and S. Ali. "Study of transition metal ion doped CdS nanoparticles for removal of dye from textile wastewater." *Journal of Inorganic and Organometallic Polymers and Materials*, **30**:1915–1923, 2020. DOI: <https://doi.org/10.1007/s10904-019-01343-5>.
- [6] Z. A. Kadem, A. B. Sharba, and J. M. Jassim. "Fine control of refractive index in large-size magnetic fluids for photonics applications." *Iraqi Journal of Applied Physics*, **19**:127–132, 2023.
- [7] Z. A. Kadem, A. B. Sharba, and J. M. Jassim. "Fast-attenuation magnetic fluid-based filters with stable and variable spectra." *Iraqi Journal of Applied Physics*, **19**:257–262, 2023.
- [8] H. Ullah, Z. Haneef, A. Ahmad, I. S. Butler, R. Nasir Dara, and Z. Rehman. "MoS₂ and CdS photocatalysts for water decontamination: A review." *Inorganic Chemistry Communications*, **153**:110775, 2023. DOI: <https://doi.org/10.1016/j.inoche.2023.110775>.
- [9] S. Kumar and J. K. Sharma. "Stable phase CdS nanoparticles for optoelectronics: a study on surface morphology, structural and optical characterization." *Materials Science-Poland*, **34**:368–373, 2016. DOI: <https://doi.org/10.1515/msp-2016-003>.
- [10] X. Li, Y. Xi, Ch. Hu, and X. Wang. "Water induced size and structure phase transition of CdS crystals and their photocatalytic property." *Materials Research Bulletin*, **48**:295–299, 2013. DOI: <https://doi.org/10.1016/j.materresbull.2012.10.022>.
- [11] K. Yang, X. Li, C. Yu, D. Zeng, F. Chen, K. Zhang, W. Huang, and H. Ji. "Review on heterophase/homophase junctions for efficient photocatalysis: The case of phase transition construction." *Chinese Journal of Catalysis*, **40**:796–818, 2019. DOI: [https://doi.org/10.1016/S1872-2067\(19\)63290-0](https://doi.org/10.1016/S1872-2067(19)63290-0).
- [12] K. R. Sreejith, L. Gorgannezhad, J. Jin, C. H. Ooi, T. Takei, G. Hayase, H. Stratton, K. Lamb, M. Shidikiy, D. Viet Dao, and N.-T. Nguyen. "Core-shell beads made by composite liquid marble technology as a versatile microreactor for polymerase chain reaction." *Micromachines*, **11**:242, 2020. DOI: <https://doi.org/10.3390/mi11030242>.
- [13] B. S. Lekshmi, A. S. Yadav, P. Ranganathan, and S. N. Varanakkottu. "Simple and continuous fabrication of Janus liquid marbles with tunable particle coverage based on controlled droplet impact." *Langmuir*, **36**:15396–15402, 2020. DOI: <https://doi.org/10.1021/acs.langmuir.0c02988>.
- [14] N. Zhang, X. Li, Y. Wang, B. Zhu, and J. Yang. "Fabrication of magnetically recoverable Fe₃O₄/CdS/g-C₃N₄ photocatalysts for effective degradation of ciprofloxacin under visible light." *Ceramics International*, **46**:20974–20984, 2020. DOI: <https://doi.org/10.1016/j.ceramint.2020.05.158>.
- [15] A. S. Reddy and J. Kim. "An efficient g-C₃N₄-decorated CdS-nanoparticle-doped Fe₃O₄ hybrid catalyst for an enhanced H₂ evolution through photoelectrochemical water splitting." *Applied Surface Science*, **513**:145836, 2020. DOI: <https://doi.org/10.1016/j.apsusc.2020.145836>.
- [16] G. Thirumala Rao and R. V. S. S. N. Ravikumar. "Novel Fe-doped ZnO-CdS nanocomposite with enhanced visible light-driven photocatalytic performance." *Materials Research Innovations*, **25**:215–220, 2021. DOI: <https://doi.org/10.1080/14328917.2020.1774726>.
- [17] Z. K. Heiba, M. B. Mohamed, and A. Badawi. "Structure, optical and electronic characteristics of iron-doped cadmium sulfide under nonambient atmosphere." *Applied Physics A*, **127**:1–11, 2021. DOI: <https://doi.org/10.1007/s00339-021-04293-3>.
- [18] A. Samadi-Maybodi, M. R. Shariati, and A. H. Colagar. "Magnetically Separable Fe₃O₄@CdS Type-II nanohybrids with excellent photocatalytic activity and antibacterial properties." *ChemPlusChem*, **83**:769–779, 2018. DOI: <https://doi.org/10.1002/cplu.201800315>.
- [19] Ch. Deng and X. Tian. "Facile microwave-assisted aqueous synthesis of CdS nanocrystals with their photocatalytic activities under visible lighting." *Materials Research Bulletin*, **48**:4344–4350, 2013. DOI: <https://doi.org/10.1016/j.materresbull.2013.07.019>.
- [20] A. Balachandran, S. P. Sreenilayam, K. Madanan, S. Thomas, and D. Brabazon. "Nanoparticle production via laser ablation synthesis in solution method and printed electronic application-A brief review." *Results in Engineering*, **16**:100646, 2022. DOI: <https://doi.org/10.1016/j.rineng.2022.100646>.
- [21] A. N. Abd, R. A. Ismail, and N. F. Habubi. "Characterization of CdS nanoparticles prepared by laser ablation in methanol." *Journal of Materials Science: Materials in Electronics*, **26**:9853–9858, 2015. DOI: <https://doi.org/10.1007/s10854-015-3660-5>.
- [22] F. H. Alkallas, S. M. Alghamdi, A. N. Al-Ahmadi, A. B. Gouider Trabelsi, E. A. Mwafy, W. B. Elsharkawy, E. Alsubhe, A. M. Mostafa, and R. A. Rezk. "Photodetection properties of CdS/Si heterojunction prepared by pulsed laser ablation in DMSO solution for optoelectronic application." *Micromachines*, **14**:1546, 2023. DOI: <https://doi.org/10.3390/mi14081546>.
- [23] A. C. Kuriakose, V. P. N. Nampoori, and S. Thomas. "Facile synthesis of Au/CdS core-shell nanocomposites using laser ablation technique." *Materials Science in Semiconductor Processing*, **101**:124–130, 2019. DOI: <https://doi.org/10.1016/j.mssp.2019.05.030>.

- [24] A. C. Kuriakose, V. P. N. Nampoori, and S. Thomas. "Influence of laser ablated Ag core on the thermo-optic and photocatalytic characteristics of CdS nanocolloids. ". *Materials Chemistry and Physics*, **258**:123911, 2021. DOI: <https://doi.org/10.1016/j.matchemphys.2020.123911>.
- [25] A. C. Kuriakose, U. Sony, V. P. N. Nampoori, and S. Thomas. "Modulation of nonlinear optical properties in CdS based core shell nanocolloids fostered by metal nanoparticles. ". *Optics & Laser Technology*, **134**:106626, 2021. DOI: <https://doi.org/10.1016/j.optlastec.2020.106626>.
- [26] M. H. Mahdiah and B. Fattahi. "Size properties of colloidal nanoparticles produced by nanosecond pulsed laser ablation and studying the effects of liquid medium and laser fluence. ". *Applied Surface Science*, **329**:47–57, 2015. DOI: <https://doi.org/10.1016/j.apsusc.2014.12.069>.
- [27] A. R. Zanatta. "Revisiting the optical bandgap of semiconductors and the proposal of a unified methodology to its determination. ". *Scientific Reports*, **9**:11225, 2019. DOI: <https://doi.org/10.1038/s41598-019-47670-y>.
- [28] S. Wageh and M. Maize. "Structure and optical properties of capped and uncapped CdS nanoparticles prepared in aqueous medium.". *Journal of Materials Science: Materials in Electronics*, **25**:4830–4840, 2014. DOI: <https://doi.org/10.1007/s10854-014-2240-4>.
- [29] S. Baral, A. Fojtik, H. Weller, and A. Henglein. "Photochemistry and radiation chemistry of colloidal semiconductors. 12. Intermediates of the oxidation of extremely small particles of cadmium sulfide, zinc sulfide, and tricadmium diphosphide and size quantization effects (a pulse radiolysis study). ". *Journal of the American Chemical Society*, **108**:375–378, 1986. DOI: <https://doi.org/10.1021/ja00263a005>.
- [30] P. Ghoranneviss, D. Dorranean, and A. H. Sari. "Effects of laser fluence on the Cd (OH)₂/CdO nanostructures produced by pulsed laser ablation method. ". *Optical and Quantum Electronics*, **51**:88, 2019. DOI: <https://doi.org/10.1007/s11082-019-1809-9>.
- [31] A. M. Darwish, W. H. Eisa, A. A. Shabaka, and M. H. Talaat. "Investigation of factors affecting the synthesis of nano-cadmium sulfide by pulsed laser ablation in liquid environment.". *Spectrochimica Acta Part A: Molecular and Biomolecular Spectroscopy*, **153**:315–320, 2016. DOI: <https://doi.org/10.1016/j.saa.2015.08.007>.
- [32] A. S. Altowyan, A. M. Mostafa, and H. A. Ahmed. "Effect of liquid media and laser energy on the preparation of Ag nanoparticles and their nanocomposites with Au nanoparticles via laser ablation for optoelectronic applications.". *Optik*, **241**:167217, 2021. DOI: <https://doi.org/10.1016/j.ijleo.2021.167217>.
- [33] M. H. Mahdiah and B. Fattahi. "Size properties of colloidal nanoparticles produced by nanosecond pulsed laser ablation and studying the effects of liquid medium and laser fluence. ". *Applied Surface Science*, **329**:47–57, 2015. DOI: <https://doi.org/10.1016/j.apsusc.2014.12.069>.
- [34] A. H. Attallah, F. S. Abdulwahid, Y. A. Ali, and A. J. Haider. "Effect of liquid and laser parameters on fabrication of nanoparticles via pulsed laser ablation in liquid with their applications: a review. ". *Plasmonics*, **18**:1307–1323, 2023. DOI: <https://doi.org/10.1007/s11468-023-01852-7>.
- [35] S. C. Singh, H. Zeng, C. Guo, and W. Cai. "Lasers: fundamentals, types, and operations. ". *Wiley*, , 2012. DOI: <https://doi.org/10.1002/9783527646821>.
- [36] J. Li, W. Zhang, H. Zheng, J. Gao, and C. Jiang. "Reducing plasma shielding effect for improved nanosecond laser drilling of copper with applied direct current. ". *Optics & Laser Technology*, **163**:109372, 2023. DOI: <https://doi.org/10.1016/j.optlastec.2023.109372>.
- [37] M. Stafe, A. Marcu, and N. N. Puscas. "Pulsed laser ablation of solids. ". *Springer*, **10**:978–3, 2014. DOI: <https://doi.org/10.1007/978-3-642-40978-3>.
- [38] A. N. Volkov and M. A. Stokes. "Effects of nanoparticles on plasma shielding at pulsed laser ablation of metal targets.". *High-Power Laser Ablation VIII*, **2310**:12939, 2024. DOI: <https://doi.org/10.1117/12.3012969>.
- [39] A. Sankhla, R. Sharma, R. S. Yadav, D. Kashyap, S. L. Kothari, and S. Kachhwaha. "Biosynthesis and characterization of cadmium sulfide nanoparticles—an emphasis of zeta potential behavior due to capping. ". *Materials Chemistry and Physics*, **170**:44–51, 2016. DOI: <https://doi.org/10.1016/j.matchemphys.2015.12.017>.
- [40] K. Wu, H. Zhu, Z. Liu, W. Rodríguez-Córdoba, and T. Lian. "Ultrafast charge separation and long-lived charge separated state in photocatalytic CdS–Pt nanorod heterostructures. ". *Journal of the American Chemical Society*, **134**:10337–10340, 2012. DOI: <https://doi.org/10.1021/ja303306u>.
- [41] G. G. Yordanov, E. Adachi, and C. D. Dushkin. "Growth kinetics and characterization of fluorescent CdS nanocrystals synthesized with different sulfur precursors in paraffin hot-matrix.". *Colloids and Surfaces A: Physicochemical and Engineering Aspects*, **289**:118–125, 2006. DOI: <https://doi.org/10.1016/j.colsurfa.2006.04.019>.
- [42] E. M. Semenova, S. A. Vorobyova, and A. I. Lesnikovich. "Interphase synthesis of Fe₃O₄/CdS core–shell nanoparticles. ". *Optical Materials*, **34**:99–102, 2011. DOI: <https://doi.org/10.1016/j.optmat.2011.07.008>.

- [43] H. A. Majeed and A. B. Sharba. “Environment-induced effects on the nonlinear refractive index of methyl orange at different spectral regions.”. *Journal of Physics: Conference Series*, **1818**: 012131, 2021. DOI: <https://doi.org/10.1088/1742-6596/1818/1/012131>.
- [44] A. B. Sharba, R. T. Ahmed, and S. F. Haddawi. “A comprehensive linear and nonlinear study on a fluorescent stain.”. *Journal of Nonlinear Optical Physics & Materials*, **31**:2250020, 2022. DOI: <https://doi.org/10.1142/S0218863522500205>.